

High-temperature ferromagnetism in epitaxial (In,Mn)Sb filmsN. D. Parashar,¹ N. Rangaraju,¹ V. K. Lazarov,² S. Xie,¹ and B. W. Wessels^{1,*}¹*Department of Materials Science and Engineering and Materials Research Center, Northwestern University, Evanston, Illinois 60208, USA*²*Department of Physics, University of York, Heslington YO10 5DD, United Kingdom*

(Received 31 August 2009; revised manuscript received 18 January 2010; published 16 March 2010)

We report ferromagnetism in single phase, epitaxial $\text{In}_{1-x}\text{Mn}_x\text{Sb}$ alloy films, with $x \leq 0.035$, grown by metalorganic vapor phase epitaxy. The alloy films exhibit well-defined magnetization versus magnetic field hysteresis loops from 4–298 K. High-field magnetotransport measurements indicated that the Hall resistivity has a nonlinear dependence on magnetic field. Ferromagnetism is supported by observation of an anomalous Hall effect and clear hysteresis in the anomalous Hall resistivity versus magnetic field measurements. Zero field cooled and field cooled magnetization measurements show reversibility indicating absence of second phase precipitates. The temperature dependence of the magnetization is described by a modified Brillouin function with a T_C of 590 K. The observed magnetic and magnetotransport properties are attributed to carrier mediated ferromagnetism involving Mn and its complexes that form shallow or resonant electronic states through correlated substitution in the semiconductor host.

DOI: [10.1103/PhysRevB.81.115321](https://doi.org/10.1103/PhysRevB.81.115321)

PACS number(s): 73.61.Ey, 75.50.Pp, 81.05.Ea

I. INTRODUCTION

Dilute (III, Mn)V ferromagnetic semiconductors (DMS) have gained significant attention in recent years for their potential application in spintronics including spin transistors, reconfigurable logic devices and magnetic field sensors.¹ For most practical applications a Curie temperature in excess of 300 K is required. While wide band-gap semiconductors, such as GaMnN, have been predicted to have high-Curie temperatures, Mn forms deep levels in these alloys that reduce the free-carrier concentration that quenches the carrier mediated ferromagnetism.^{2,3} Narrow gap (III, Mn)V semiconductors, have Mn acceptor levels that are shallow or resonant with the valence band, but have been predicted from mean field theory to have a low-Curie temperature. Nevertheless the material remains highly conducting even when heavily doped with manganese, which should favor carrier mediated ferromagnetism.⁴ Previously, we have reported that nominally phase pure narrow gap InMnAs alloys with an exceptionally high T_C of 330 K could be achieved when grown by metal-organic vapor phase epitaxy (MOVPE).^{5,6} While details of the origin of the ferromagnetism in the alloy system grown by this technique are not well understood, the source of the localized spins has been attributed to atomic scale complexes resulting from correlated substitution of magnetic impurities.⁷ The complexes consist of Mn substituting on near neighbor cation sites forming magnetic dimers ($\text{Mn}_{\text{In}}\text{-Mn}_{\text{In}}$) and trimers. These Mn complexes can participate in exchange p - d coupling with free holes that lead to an enhanced Curie temperature.⁸ Recently, enhancement in Curie temperatures has been reported for other alloy systems upon formation of nanoscale ferromagnetic clusters.⁹

The question arises as to whether or not there are other suitably doped narrow gap III–V semiconductors with even higher Curie temperatures.¹⁰ One system of interest is InMnSb where Mn forms a shallow acceptor level in InSb.^{11,12} However, as in the case of InMnAs, Mn has limited solubility and can form magnetic precipitates in the alloy.^{11,12} Prior

work on this alloy has been centered on thin films grown by low-temperature (LT) molecular beam epitaxy (MBE)^{13,14} and liquid phase epitaxy.¹⁵ The T_C of the MBE films, however is very low, less than 8 K. Here, we report on the observation of high temperature ferromagnetism in InMnSb semiconductor films prepared by MOVPE. The alloy is phase pure as determined by double-crystal x-ray diffraction (DCXRD) and transmission electron microscopy (TEM). The Curie temperature is in excess of 400 K as determined by magnetization measurements. The alloy also exhibits anomalous Hall effect over the temperature range of 4–298 K. This work indicates that narrow gap III–V semiconductors are suitable hosts to achieve high- T_C materials for spintronic devices.

II. EXPERIMENTAL

$\text{In}_{1-x}\text{Mn}_x\text{Sb}$ films were grown on GaAs (100) substrates using atmospheric pressure metalorganic vapor phase epitaxy (MOVPE) in a system described earlier.¹⁶ Alloys were grown at a substrate temperature of 400 °C at a typical growth rate of 330 nm/hr. The film thickness was ~ 350 nm. The films were p -type with resistivity of $\sim 2 \times 10^{-3} \Omega \text{ cm}$ and nominal hole concentration of $1\text{--}2.6 \times 10^{19} \text{ cm}^{-3}$ as determined by high-field Hall measurements. The manganese concentration was determined by energy dispersive x-ray analysis (EDS) using a beam energy of 25 keV and a probe current of 30 mA. The crystalline quality, phase purity and the lattice constant of the InMnSb films were determined by double crystal x-ray diffraction using Cu $K\alpha_1$ radiation. TEM analysis was made with a JEOL 2100 FasTEM and JEOL 3000F TEM, which were operated at 200 and 300 kV, respectively. Field dependence of magnetization of InMnSb films was measured with a SQUID (Quantum Design MPMS-5) magnetometer. Local structure of Mn was determined using extended x-ray absorption extra fine structure (EXAFS) measurements carried out at Sector 5 BMD beamline at advanced photon source (APS).

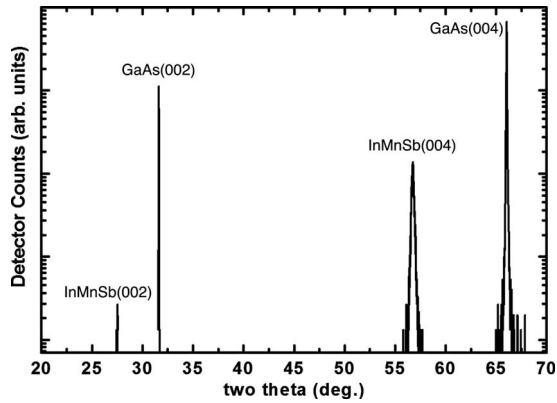


FIG. 1. (a) $\theta-2\theta$ XRD scans for $\text{In}_{0.98}\text{Mn}_{0.02}\text{Sb}/\text{GaAs}$ film.

III. RESULTS

A. Structural properties

Figure 1 shows the $\theta-2\theta$ x-ray diffraction curve for a $\text{In}_{0.98}\text{Mn}_{0.02}\text{Sb}$ film grown on a GaAs substrate. InMnSb (002) and (004) diffraction peaks can be seen in the $\theta-2\theta$ scan along with GaAs (002) and (004) substrate reflection peaks. No evidence of any other second phase precipitate such as MnSb , which has a nickel arsenide structure, was detected by x-ray diffraction. The full width at half maximum (FWHM) of the rocking curve of $\text{In}_{0.98}\text{Mn}_{0.02}\text{Sb}$ film was 0.14° , indicating good crystalline quality despite of the large lattice mismatch of 12 per cent between the film and GaAs substrate. Figure 2(a) top image shows the high-resolution TEM image of a $\text{In}_{0.98}\text{Mn}_{0.02}\text{Sb}$ film grown on a GaAs substrate. The bottom image is a high resolution TEM image at the $\text{In}_{0.98}\text{Mn}_{0.02}\text{Sb}/\text{GaAs}$ interface. The film forms a nearly atomically abrupt interface with the substrate. The right inset is the selected area diffraction pattern of the cross-section. Clear fourfold symmetry can be seen in the diffraction pattern, which is the characteristic Zinc Blende structure. No evidence of secondary phase (with hexagonal symmetry) is observed by high-resolution TEM for the InMnSb layer, which is consistent with the x-ray diffraction analysis. Figure 2(b) shows an EDX line scan across the film indicating no Mn segregation at a 10 nm length scale and a constant integrated intensity ratio of Mn/Sb and In/Sb in the film and the interface.

To ascertain whether the dopant manganese ions in the alloy substitute on to the cation lattice site of the host, and not form secondary ferromagnetic phases, x-ray absorption spectroscopy (XAS) measurements were done. The x-ray absorption near edge structure (XANES) measurements obtained at the Mn K -edge indicates that Mn is in a 2^+ charge state. Fourier transformed EXAFS, $|\chi(R)|$, of $\text{In}_{0.965}\text{Mn}_{0.035}\text{Sb}$ film for Mn K -edge, measured at room temperature shows that the first atomic interaction peak in the Mn K -edge radial distribution function (RDF) is well accounted for, including the satellite peaks, by assuming four Sb near neighbor atoms (Fig. 3). Preliminary EXAFS analysis also supports Mn having a 2^+ charge state. Furthermore, EXAFS analysis indicates that Mn substitutes on tetrahedral cation sites, replacing In in the zinc blende lattice.¹⁷

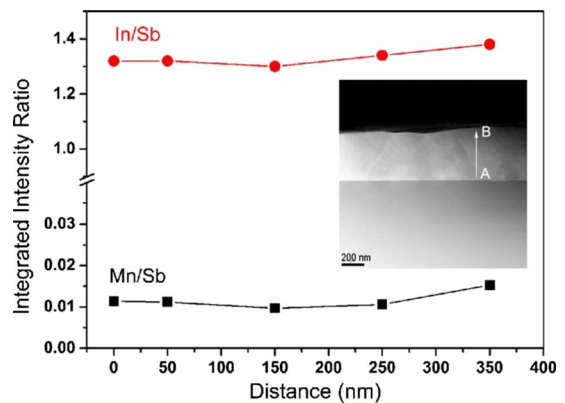
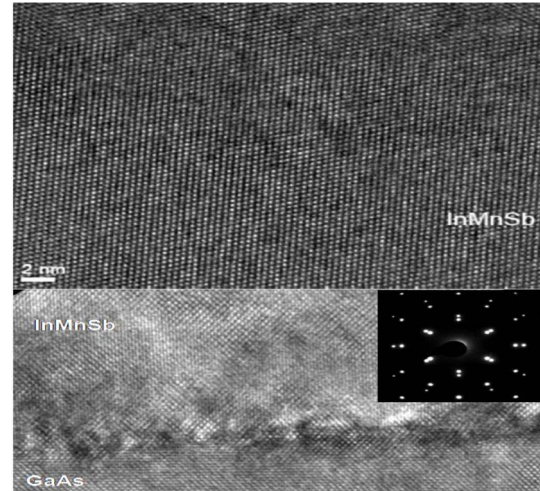


FIG. 2. (Color online) (a) High-resolution TEM image of a $\text{In}_{0.98}\text{Mn}_{0.02}\text{Sb}$ film grown on GaAs substrate; inset: left—cross-section image showing $\text{InMnSb}/\text{GaAs}$ film-substrate interface, right—selected area diffraction pattern showing fourfold symmetry. (b) EDX line scan across the $\text{InMnSb}/\text{GaAs}$ interface showing In/Sb, Mn/Sb atomic ratio as a function of distance across the film.

B. Field dependence of magnetization

To determine the magnetic properties of the alloys, the magnetization was measured as a function of applied magnetic field. Figure 4 plots the magnetic field dependence of the magnetization for two alloy films, with $x=0.02$ and 0.035 , measured at 298 K, where the magnetic field was applied in-plane. For analysis, the diamagnetic contribution from the substrate was subtracted. Well-resolved hysteresis loops are observed at room temperature. For $\text{In}_{0.98}\text{Mn}_{0.02}\text{Sb}$ film, the measured saturation magnetization (M_s) is 4.5 emu/cm^3 with a remanence (M_r) of 1.6 emu/cm^3 and a coercive field (H_c) of 217 G. For $\text{In}_{0.965}\text{Mn}_{0.035}\text{Sb}$ film the values of M_s and M_r increase to 22 and 4.6 emu/cm^3 , respectively. The value of 22 emu/cm^3 for M_s corresponds to $2.28\mu_B$ Bohr magnetons per Mn.

C. Magnetotransport measurements

The presence of ferromagnetism in the alloy is supported by Hall effect measurements. The total Hall resistivity $\rho_{xy}(=\rho_H)$, for ferromagnetic materials can be described as a sum of two terms, $\rho_H=\rho_{xy}=\rho_{OH}+\rho_{AH}=R_O B+R_A M$, where

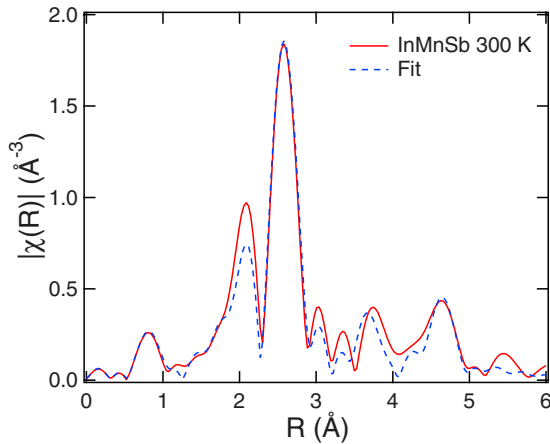


FIG. 3. (Color online) Fourier transformed EXAFS, $|\chi(R)|$, of $\text{In}_{0.98}\text{Mn}_{0.02}\text{Sb}$ film for Mn K edge, measured at room temperature. The first atomic interaction peak in the Mn K edge radial distribution function (RDF) is well accounted for, including the satellite peaks, by assuming four Sb near neighbor atoms.

ρ_{OH} is the normal Hall contribution, ρ_{AH} is the anomalous Hall contribution, B is the applied magnetic field, M is the magnetization and R_o and R_A are the ordinary and anomalous Hall coefficients, respectively.¹⁸ The normal Hall contribution results from the Lorentz force which is proportional to the external magnetic field B , ($R_o=1/pe$). The second component, the anomalous Hall contribution is proportional to the magnetization M , and is attributed to scattering processes involving spin-orbit interactions.^{19,20} In ferromagnetic semiconductors at low magnetic fields, the Lorentz force term gives a negligible contribution compared to the anomalous Hall term.¹⁸ Thus, in the low-magnetic field regime, the Hall resistivity is proportional to the magnetization. Since for a nonmagnetic semiconductor the Hall resistivity is linear in magnetic field, a nonzero value of R_A indicates the films are ferromagnetic.¹⁸ Furthermore, the observation of both AHE and well-resolved hysteresis loops is attributed to the presence of carrier-mediated ferromagnetism.²¹

Figure 5(a) shows Hall resistivity (ρ_{Hall}) versus magnetic field for $\text{In}_{0.98}\text{Mn}_{0.02}\text{Sb}$ film measured between 1.4–298 K, for an applied magnetic field of ± 18 T. From Fig. 5(a) we can clearly see that the Hall resistivity has a nonlinear de-

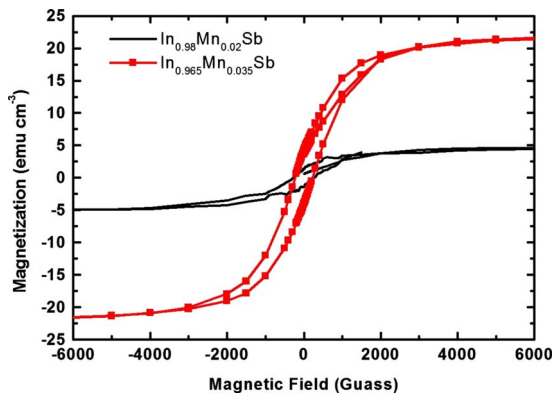
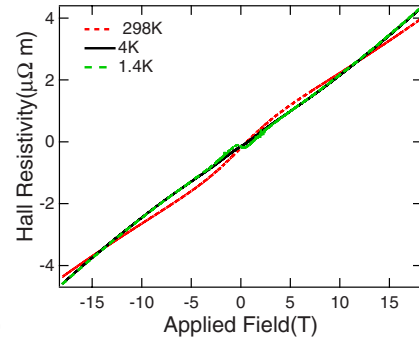
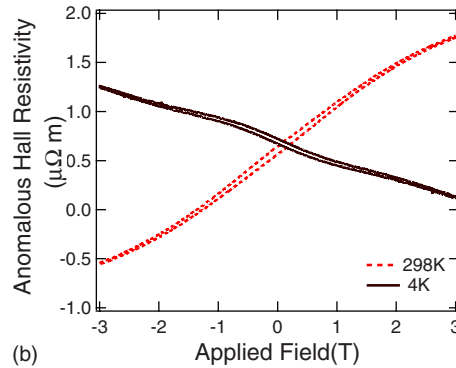


FIG. 4. (Color online) Room temperature ferromagnetic hysteresis curves for two $\text{In}_{1-x}\text{Mn}_x\text{Sb}$ films.



(a)



(b)

FIG. 5. (Color online) (a) Hall resistivity versus magnetic field for $\text{In}_{0.98}\text{Mn}_{0.02}\text{Sb}$ film measured at 1.4, 4, 298 K, for -18 to 18 T. (b) Low field anomalous Hall resistivity versus magnetic field data from Fig. 5(a).

pendence on magnetic field indicating the presence of anomalous Hall effect (AHE). To better resolve the AHE, the ordinary Hall component was removed. Removing ordinary Hall component from the high-field region ensures that magnetization is saturated. To remove the linear contribution originating from the ordinary Hall component of Hall resistivity, straight lines were fit to the experimental data between 15 and 18 T, where contribution from AHE are minimal. The anomalous Hall resistivity was calculated by removing the product of the obtained slope and applied field from the Hall resistivity. Figure 5(b) shows the temperature dependence of anomalous Hall resistivity for magnetic field range of -3 – 3 T for 4 and 298 K. Clear hysteresis can be seen at both 298 and 4 K. The magnitude of hysteresis in the anomalous Hall resistivity is small because the magnetic field is applied along the hard axis (out-of-plane) of magnetization in the film.

The observation of anomalous Hall effect, at room temperature, indicates the presence of spin-orbit coupling which induces anisotropy between the scattering of spin-up and spin-down carriers by the impurities.²² Furthermore, it establishes the presence of spin polarized carriers in the film.¹⁸ A nonzero anomalous Hall coefficient can result from a carrier scattering mechanism like side jump and skew scattering of the carriers.^{19,20} The presence of a hysteresis loop, in both magnetization and anomalous Hall resistivity measurements, at room temperature indicates that the film is ferromagnetic at room temperature. Thus the data analysis indicates that the hysteresis in the InMnSb film is due to carrier mediated ferromagnetism and does not result from isolated ferromagnetic precipitates such as MnSb .²³

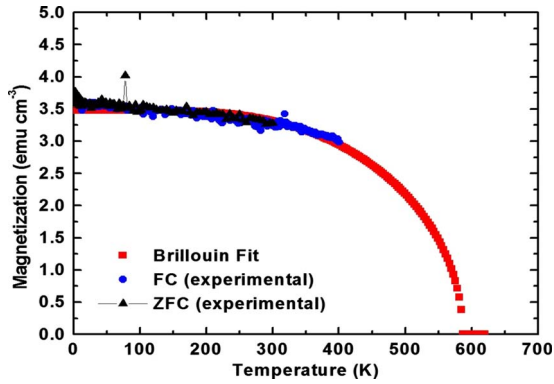


FIG. 6. (Color online) ZFC/FC magnetization versus temperature curve for $\text{In}_{0.98}\text{Mn}_{0.02}\text{Sb}$ film for the temperature range 2–400 K for an applied field of 500 G. ● FC, ▲ ZFC, ■ Brillouin function fit after Bean and Rodbell (Ref. 26)

D. Temperature dependence of magnetization

To determine the nature of the observed ferromagnetism the temperature dependence of the magnetization for the $\text{In}_{0.98}\text{Mn}_{0.02}\text{Sb}$ film was measured from 4 to 400 K for two different sets of conditions, field cooled (FC) and zero field cooled (ZFC). In the FC measurement, a magnetic field of 500 G is applied at 298 K, and then the sample is cooled to 4 K. Next, the M versus T curve is measured with increasing temperature, as in Fig. 6. The sample was subsequently measured under a ZFC condition, where the sample is first cooled from 298 to 4 K without a magnetic field. A small magnetic field of 500 G is then applied at 4 K, following which the M versus T curve is measured as the temperature increases from 4 to 298 K.²⁴ Figure 6 shows the magnetization versus temperature curves for ZFC and FC measurements for $\text{In}_{0.98}\text{Mn}_{0.02}\text{Sb}$ film, after removing the diamagnetic contribution from the substrate. A clear reversibility is observed between the FC and ZFC curves. Since the two curves are coincident, this indicates that $\text{In}_{0.98}\text{Mn}_{0.02}\text{Sb}$ is a homogeneous ferromagnet with no nanoscale second phase magnetic precipitates, except potentially those with a blocking temperature in excess of 400 K.²⁵ The observation of reversible ZFC/FC curves is consistent with the findings from XRD and TEM measurements that indicated absence of any second phase magnetic impurity precipitates (e.g., MnSb).

The magnetization is only weakly temperature dependent over the temperature range of 4–400 K as shown in Fig. 6. The temperature dependence of the magnetization was calculated using a mean field model after Bean and Rodbell.^{6,26} The temperature dependence of magnetization, for $j=1/2$, is given by $T/T_o = (\sigma/\tanh^{-1}\sigma)(1 + \eta\sigma^2/3 - PK\beta)$ where $\eta \equiv \frac{3}{2}NkKT_o\beta^2$, where σ is the reduced magnetization, η is a fitting parameter ($\eta < 1$ for a second order transition, $\eta=0$ equation reduces to a Brillouin function, $\eta > 1$ for a first order transition), β is the slope of the dependence of Curie temperature on volume, T_o is the Curie temperature for an uncompressed lattice, K is the compressibility, T is the temperature and P is the pressure, respectively. As shown in Fig. 6 there is excellent agreement between theory and experiment taking $\eta=0$ over the temperature range of 4–400 K. A

T_C of 590 K is extrapolated from the mean field model and the FC data.

IV. DISCUSSION

The large transition temperature for the InMnSb is in contrast to predictions based on an existing mean field theory of carrier mediated ferromagnetism for a random solid solution. Indeed, previous theoretical calculations using a Rudermann-Kittel-Kasuya-Yosida (RKKY) model predicted a temperature of 10 K.^{2,27} The high-Curie temperature experimentally observed in the present study suggests that other mechanisms should be considered. One possibility is that phase separation occurs and MnSb precipitates form, stabilizing the ferromagnetism in the dilute InMnSb alloy. Hexagonal MnSb is ferromagnetic with a T_C of 570 K.¹² X-ray diffraction, EXAFS analysis, and TEM, in the present study however, indicated no evidence of a hexagonal phase in the alloy within detection limits of the analysis techniques. Further evidence for the absence of hex-MnSb in MOVPE InMnSb films has been demonstrated by recent x-ray magnetic circular dichroism (XMCD) studies.²⁸ A clear difference in the XMCD line shape of MOVPE InMnSb and hex-MnSb films is measured, which arises due to the difference in crystal symmetry and coordination of Mn. Thus if present, it has been proposed that MnSb could be potentially incorporated as clusters with tetrahedral symmetry although MnSb in a zinc blende structure is metastable.²⁹ Furthermore, zinc blende MnSb, if present as incoherent precipitates should be observable by x-ray diffraction since its calculated lattice constant using first principle calculations is 6.203 Å, which is much less than the value of 6.48 Å of dilute InMnSb .³⁰ Since neither x-ray diffraction nor TEM indicated the presence of an incoherent zinc blende MnSb phase, the MnSb clusters, if present, must be coherent with a lattice constant comparable to InSb . Furthermore, they must be of atomic dimensions since the ZFC/FC magnetization measurements indicated the alloy is homogeneous.²⁵ The lack of second phase precipitates indicates that other mechanisms for the ferromagnetism are more likely.

Nevertheless, MnSb phase segregation has been observed in other (III,Mn)Sb alloys. MnSb phase segregation has been reported in GaMnSb alloys grown by MBE.³¹ While the alloys deposited at 560 °C [HT-(Ga,Mn)Sb] showed the presence of MnSb second phase, those grown at low temperatures (250 and 300 °C) [LT-(Ga,Mn)Sb] showed coexisting (Ga,Mn)Sb and MnSb phases. HT-(Ga,Mn)Sb films exhibited ferromagnetism from 5–320 K with a weak temperature dependence of magnetization that was attributed to MnSb phase.³¹ The Hall resistance of the films was reported to have a linear dependence on B for temperature >40 K and a non-linear dependence on B for temperatures <40 K, that was attributed to the ZB (Ga,Mn)Sb low-temperature ferromagnetic phase. LT-(Ga,Mn)Sb on the hand, was superparamagnetic for 5–300 K with no hysteresis and no magnetic anisotropy. The AHE was found to be proportional to the magnetization of ZB-(Ga,Mn)Sb. Clearly magnetization and AHE findings for the MOVPE grown InMnSb are dissimilar to that of GaMnSb films with MnSb precipitates. InMnSb is

ferromagnetic with well-defined hysteresis, and nonlinear dependence on B of AHE.

The large transition temperature of MOVPE grown films (>400 K) is in contrast to the previously reported values for LT-MBE InMnSb films (<10 K).¹³ This difference in T_C is tentatively attributed to the difference in deposition temperature, which in turn changes the kinetics of growth. LT-MBE InMnSb films are deposited at growth temperature of 170 °C, whereas MOVPE films are deposited at growth temperature of 400 °C. The kinetics of the LT-MBE growth leads to random distribution of Mn atoms in the InSb host matrix. Whereas in MOVPE grown films Mn incorporates as Mn-related tetrahedrally coordinated clusters (dimers, trimers etc), which are of the order of 1nm or less in size as has been previously shown using EXAFS studies.⁷ This difference in microstructure changes the material properties, including T_C and carrier concentration. For example, in LT-MBE grown film with 0.028 Mn% the reported values of saturation magnetization and carrier concentration are 6 emu/cm³ and 2.1×10^{20} cm⁻³, respectively.¹³ For MOVPE grown film with 0.02 Mn% the measured saturation magnetization and carrier concentration values are 5 emu/cm³ and 2.6×10^{19} cm⁻³, respectively. This difference in carrier concentration value, by one order of magnitude, is attributed to the distribution of Mn in these two types of films. For LT-MBE films each substitutional dopant Mn dopes the host with one hole. Whereas for MOVPE films the holes localize within the cluster, this localization reduces the free-carrier concentration. There is both experimental⁸ and theoretical evidence that clusters result in reduced carrier concentration.³² Raebinger *et al.* showed that cluster formation lowers the carrier concentration. The hole concentration is reduced by $1/n$ where n is the number of Mn atoms in the cluster.³²

As for possible mechanisms stabilizing the ferromagnetism in the MOVPE films, stabilization of ferromagnetism by a double exchange or superexchange mechanisms via percolation has been previously proposed as a possible mechanism for other DMS.³³ The concentration of Mn of 0.02 in the InMnSb alloy, however, is too low to form a percolative pathway. Nevertheless the ZFC/FC magnetization measurements indicate that there is sufficient intercluster coupling to stabilize ferromagnetism up to 590 K.

This leads us to propose that the ferromagnetism in InMnSb is stabilized by an RKKY mechanism and with correlated substitution of magnetic impurities.³⁴ In this case, substitutional Mn is the source of free holes but Mn acceptor complexes are the source of the localized spins that lead to a high T_C . There is both theoretical and experimental evidence for transition metals forming complexes including dimers and trimers in other III–V semiconductor alloys.⁶ From statistical arguments they are expected even in random alloys at the high concentrations used. We have observed Mn complexes in InMnAs by EXAFS analysis.⁷ Furthermore Raebinger *et al.* have shown for GaMnAs using first principles calculations that these complexes are stable, electronically active and have large magnetic moments.³² Meilikhov showed using mean field theory with RKKY interactions that magnetic ion clustering shifts the ferromagnetic stability range toward a lower magnetic impurity concentration.³⁴

Thus, correlated substitution of magnetic impurities may be the origin of the high T_C . As aforementioned presumably formation of these complexes is favored in the MOVPE deposition process and not in LT-MBE process.

As to the intercluster coupling, an RKKY mechanism where free holes mediate the ferromagnetism is indeed favored in narrow band-gap semiconductors. The free holes in these materials have a small effective mass m^* , which favors a long interaction distance and effective exchange coupling. Indeed, the calculated hole Bohr radius, $a_o = (\hbar^2/2m^*E_a^0)^{1/2}$, for an ionization energy $E_a^0 = 7$ meV is 40 Å in Mn doped InSb.^{11,35} This radius is large enough so that there is sufficient overlap of the Mn derived hole wave functions to stabilize ferromagnetism even for a Mn concentration of several percent. Percolation would not be needed.

As to the extrapolated T_C of the alloy being similar to that of the parent magnetic compound MnSb, there is growing experimental and theoretical evidence for its occurrence. For MOVPE grown InMnAs, the measured T_C is 330 K compared to 320 K for MnAs.^{6,10} Furthermore, Franceschetti *et al.* have shown using first principles calculations and a cluster expansion that artificial magnetic semiconductor structures have T_C 's that approaches the binary magnetic parent compound.³⁶ For example, for GaMnAs a T_C of the order of 350 K was predicted for a number of compounds that is comparable to the experimental value of 320 K for MnAs.

V. CONCLUSIONS

In summary, single phase InMnSb epitaxial films, grown by MOVPE are ferromagnetic with a T_C in excess of 400 K. ZFC/FC magnetization versus temperature curves show clear reversibility supporting the homogenous nature of ferromagnetism in the films. Well defined hysteresis loops are observed at room temperature as indicated by magnetization measurements, indicative of ferromagnetic order. Furthermore, the presence of an AHE with clearly resolved ρ_{Hall} versus H hysteresis loops support the assignment of ferromagnetic order. Using a mean field model to describe the magnetic interaction, a T_C of 590 K was calculated. In contrast to earlier theoretical predictions, this work indicates that narrow band-gap III–V semiconductors are excellent hosts for obtaining high- T_C ferromagnetic semiconductors.

ACKNOWLEDGMENTS

This work is supported by the National Science Foundation (NSF) under Grant No. DMR—0804479. V. K. Lazarov acknowledges support from RAEng and EPSRC at Oxford University. X-ray diffraction analysis was performed at the J. B. Cohen x-ray diffraction facility supported by the MRSEC program of the NSF (Grant No. DMR-0520513) at the Materials Research Center (MRC) of Northwestern University. EDS analysis was done at the EPIC facility of NUANCE

Center at Northwestern University. The microscopy research was supported by the MRSEC program of the NSF (Grant No. DMR-0520513) at the MRC of Northwestern University; and performed in the EPIC facility of NUANCE Center at Northwestern University. AHE measurements were per-

formed at the National High Magnetic Field Laboratory, which is supported by NSF (Grant No. DMR-0654118), the State of Florida and the DOE. The authors thank Qing Ma from DNCD-CAT, Argonne National Laboratory for technical discussion regarding EXAFS experiments.

*b-wessels@northwestern.edu

- ¹S. A. Wolf, D. D. Awschalom, R. A. Buhrman, J. M. Daughton, S. von Molnar, M. L. Roukes, A. Y. Chtchelkanova, and D. M. Treger, *Science* **294**, 1488 (2001).
- ²T. Dietl, H. Ohno, F. Matsukura, J. Cibert, and D. Ferrand, *Science* **287**, 1019 (2000).
- ³R. Y. Korotkov, J. M. Gregie, and B. W. Wessels, *Appl. Phys. Lett.* **80**, 1731 (2002).
- ⁴K. Huang and B. W. Wessels, *Appl. Phys. Lett.* **52**, 1155 (1988).
- ⁵A. J. Blattner, J. Lensch, and B. W. Wessels, *J. Electron. Mater.* **30**, 1408 (2001).
- ⁶A. J. Blattner and B. W. Wessels, *Appl. Surf. Sci.* **221**, 155 (2004); *J. Vac. Sci. Technol. B* **20**, 1582 (2002).
- ⁷Y. L. Soo, S. Kim, Y. H. Kao, A. J. Blattner, B. W. Wessels, S. Khalid, C. Sanchez Hanke, and C. C. Kao, *Appl. Phys. Lett.* **84**, 481 (2004).
- ⁸P. T. Chiu and B. W. Wessels, *Phys. Rev. B* **76**, 165201 (2007); *Appl. Phys. Lett.* **89**, 102505 (2006); **86**, 072505 (2005).
- ⁹S. Kuroda, N. Nishizawa, K. Takita, M. Mitome, Y. Bando, K. Osuch, and T. Dietl, *Nature Mater.* **6**, 440 (2007).
- ¹⁰B. W. Wessels, *New J. Phys.* **10**, 055008 (2008).
- ¹¹S. A. Obukhov, *Phys. Status Solidi B* **242**, 1298 (2005).
- ¹²V. M. Novotortsev, I. S. Zakharov, A. V. Kochura, S. F. Marenkin, R. Laiho, E. Lahderanta, A. Lashkul, A. G. Veresov, A. V. Molchanov, and G. S. Yur'ev, *Russ. J. Inorg. Chem.* **51**, 1627 (2006).
- ¹³T. Wojtowicz, G. Cywinski, W. L. Lim, X. Liu, M. Dobrowolska, J. K. Furdyna, K. M. Yu, W. Walukiewicz, G. B. Kim, M. Cheon, X. Chen, S. M. Wang, and H. Luo, *Appl. Phys. Lett.* **82**, 4310 (2003).
- ¹⁴S. Yanagi, K. Kuga, T. Slupinski, and H. Munekata, *Physica E* **20**, 333 (2004).
- ¹⁵K. Ganesan, S. Mariyappan, and H. L. Bhat, *Solid State Commun.* **143**, 272 (2007).
- ¹⁶L. Q. Qian and B. W. Wessels, *Appl. Phys. Lett.* **63**, 628 (1993).
- ¹⁷N. D. Parashar, Q. Ma, and B. W. Wessels (unpublished).
- ¹⁸H. Toyosaki, T. Fukumura, Y. Yamada, K. Nakajima, T. Chikyow, T. Hasegawa, H. Koinuma, and M. Kawasaki, *Nature Mater.* **3**, 221 (2004).
- ¹⁹L. Berger, *Phys. Rev. B* **2**, 4559 (1970); **5**, 1862 (1972).
- ²⁰J. Smit, *Physica* **21**, 877 (1955); R. Karplus and J. M. Luttinger, *Phys. Rev.* **95**, 1154 (1954).
- ²¹G. Mihály, M. Csontos, S. Bordács, I. Kézsmárki, T. Wojtowicz, X. Liu, B. Jankó, and J. K. Furdyna, *Phys. Rev. Lett.* **100**, 107201 (2008).
- ²²T. Jungwirth, Q. Niu, and A. H. MacDonald, *Phys. Rev. Lett.* **88**, 207208 (2002).
- ²³It should be noted that in Fig. 5(b), there is a change of sign of AHE at temperature of 4 K. The decrease in the hysteretic behavior upon decreasing the temperature from 298–4 K is explained by the temperature dependence of the longitudinal resistance in the films. Temperature and manganese concentration dependence of Hall resistivity will be discussed, in detail, elsewhere.
- ²⁴X. X. Zhang, *Magnetic Relaxation and Quantum Tunneling of Magnetization: Handbook of Advanced Magnetic Materials* (Tsinghu University Press, New York, 2005).
- ²⁵P. N. Hai, K. Takahashi, M. Yokoyama, S. Ohya, and M. Tanaka, *J. Magn. Magn. Mater.* **310**, 1932 (2007).
- ²⁶C. P. Bean and D. S. Rodbell, *Phys. Rev.* **126**, 104 (1962).
- ²⁷T. Dietl, H. Ohno, and F. Matsukura, *Phys. Rev. B* **63**, 195205 (2001).
- ²⁸N. D. Parashar, D. J. Keavney, and B. W. Wessels, *Appl. Phys. Lett.* **95**, 201905 (2009).
- ²⁹H. M. Hong, Y. J. Kang, J. Kang, E. C. Lee, Y. H. Kim, and K. J. Chang, *Phys. Rev. B* **72**, 144408 (2005).
- ³⁰J. C. Zheng and J. W. Davenport, *Phys. Rev. B* **69**, 144415 (2004).
- ³¹E. Abe, F. Matsukura, H. Yasuda, Y. Ohno, and H. Ohno, *Physica E* **7**, 981 (2000).
- ³²H. Raebiger, A. Ayuela, and J. von Boehm, *Phys. Rev. B* **72**, 014465 (2005); *J. Phys.: Condens. Matter* **16**, L457 (2004).
- ³³K. Sato, W. Schweika, P. H. Dederichs, and H. Katayama-Yoshida, *Phys. Rev. B* **70**, 201202(R) (2004).
- ³⁴E. Z. Meilikhov, *Phys. Rev. B* **75**, 045204 (2007).
- ³⁵T. Jungwirth, J. Sinova, A. H. MacDonald, B. L. Gallagher, V. Novak, K. W. Edmonds, A. W. Rushforth, R. P. Campion, C. T. Foxon, L. Eaves, E. Olejnik, J. Masek, S. R. Eric Yang, J. Wunderlich, C. Gould, L. W. Molenkamp, T. Dietl, and H. Ohno, *Phys. Rev. B* **76**, 125206 (2007).
- ³⁶A. Franceschetti, S. V. Dudiy, S. V. Barabash, A. Zunger, J. Xu, and M. van Schilfgarde, *Phys. Rev. Lett.* **97**, 047202 (2006).